ACS Combinatorial Science

Research Article

pubs.acs.org/acscombsci

Combinatorial High-Throughput Screening for Highly Active Pd–Ir–Ce Based Ternary Catalysts in Electrochemical Oxygen Reduction Reaction

Sung Hyeon Park,[†] Chang Hyuck Choi,[†] Jae Kang Koh,[‡] Chanho Pak,[§] Seon-ah Jin,[§] and Seong Ihl Woo*[,†,‡]

[†]Department of Chemical and Biomolecular Engineering and [‡]Graduate School of EEWS (WCU), Korea Advanced Institute of Science and Technology, Daejeon 305-701, Republic of Korea

[§]Samsung Advanced Institute of Technology, Nongseo-dong, Giheung-gu, Yongin-si 446-712, Gyeonggi-do, Republic of Korea

Supporting Information

ABSTRACT: A combinatorial library having 66 different ternary compositions of Pd–Ir–Ce was prepared via the impregnation method to find the optimum ternary composition with the highest performance toward oxygen reduction reaction (ORR) in acid media. Its performance in ORR activity of the combinatorial array was evaluated through two different combinatorial high-throughput screening methods to gain validity: (1) multielectrode half-cell method and (2) optical screening method. From the combinatorial results, the spot at 79:12:9 for Pd–Ir–Ce (at. %) in the array showed the highest ORR activity. The electrochemical characterizations of the single catalyst demonstrates that the optimized $Pd_{79}Ir_{12}Ce_9/C$ catalyst shows 1.5 times the ORR activity compared to that of Pd/C catalyst at 0.85 V (vs. RHE). In the Pd–Ir–Ce based catalysts, X-ray diffraction (XRD) and X-ray photoelectron spectroscopy (XPS) results reveal that Ir and Ce are present in the form of IrO_2 and CeO_2, respectively, and the electron configuration of Pd is effectively modified through the decoration with IrO_2 and CeO_2. From the results, we suggest that the electro-modification of Pd through strong metal–metal oxide interaction with IrO_2–CeO_2 was a reason for the enhanced ORR activity.

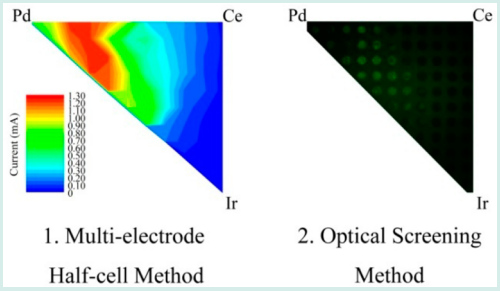

KEYWORDS: *combinatorial research, multielectrode half-cell, optical screening, Pd-based catalysts, fuel cell cathode, oxygen reduction reaction*

INTRODUCTION

Polymer electrolyte membrane fuel cells (PEMFCs) are devices regarded as an eco-friendly power source with high energy conversion efficiency and density.[1,2] This high energy conversion efficiency is due to the direct conversion of chemical energy to electrical energy, which evades the properties applying to the Carnot engine. However, for the commercialization of such device, issues regarding the high cost must be solved because Pt or Pt-derived materials have been used as electrode materials in PEMFCs. To overcome such measures, the substitution of Pt by cheaper materials should be of consideration.

Palladium is about one-third the cost of platinum, and it shows a relatively good performance toward oxygen reduction reaction (ORR).[3] However, Pd alone shows a much lower ORR activity than that of Pt; therefore, various approaches have been applied to improve the activity of Pd-based catalysts via alloying with other transition metals (e.g., Co, Ni, Fe, and Mo),[4−8] or decoration with metal oxides (e.g., WO_3, TiO_2, CeO_2, and Mn_3O_4).[9−12] Recently, the decoration by Ir (or IrO_2) or Ce (or CeO_2) has been a promising method in the modification of the Pd-derived catalysts for ORR activity.[11,13] Until now, binary compositions have been studied extensively; however, researches regarding ternary compositions have yet not been progressed in depth, even though ternary compositions could have higher potential as an ORR catalyst. Therefore, in this study, Pd-based ternary catalysts with the combination of Pd–Ir–Ce were prepared and investigated to find the optimized compositions toward ORR in acid media. However, a big drawback of such study is that it requires a vast amount of both time and labor because of the extensive variations of possible combinations and compositions.

Combinatorial screening is a highly potential methodology that can evaluate simultaneously the performance of a large number of catalyst variations; therefore, this method has been applied in various fields, such as random access memory,[14] selective catalytic reduction of NO,[15] reforming of methane,[16] and more.[17−26] In the late 1990s Reddington et al. began the application of optical screening in the field of fuel cells, and since, this methodology has been put into practice.[27] Research groups by Smotkin, Mallouk, McGinn, and others have reported this method applied to find optimized combinations

Received: January 15, 2013
Revised: August 26, 2013
Published: October 22, 2013

and compositions of catalyst having outstanding performance toward ORR.[3,13,27−39] Even in our group, we have also been using this methodology and developed various optimized catalysts for PtRuFe,[38] PdCo,[3] PtRuFeSe,[39] and more.[13] However, this methodology has few main drawbacks.

First, the diffusion of the electrolyte hindered the acute differentiation between the catalysts' performance, so the analysis was possible only for a matter of a few minutes (1−2 min). Second, an acute criterion of the brightness of each catalyst spot made it difficult to differentiate between the spots with the naked eye. Third, the analysis of the catalysts was a weighted evaluation. Therefore, in this experiment we have overcome these few main drawbacks by making a mask that could decrease the rate of diffusion of the electrolyte, allowing a longer analysis of the catalysts. Also, a second type of combinatorial method, the multielectrode half-cell method, was incorporated. This methodology has a drawback, which is, as the number of catalysts increases, the longer it takes for the evaluation of the catalysts. However, this methodology is a not weighted evaluation. Through the use of these improvements, we anticipated an upgrade in the validity of this experiment.

The two different combinatorial high-throughput screening methods are the following. First, the scheme of the multi-electrode half-cell method is shown in Figure 1. This

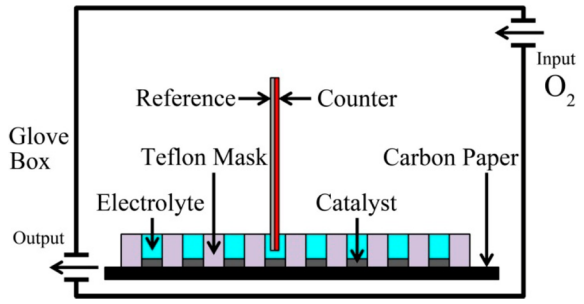

Figure 1. Scheme of the multielectrode half-cell method.

methodology requires of a working combinatorial array, a counter, and a reference electrode. The comparison of the performance of the catalysts is assessed similar to a three electrode method: each catalyst is analyzed using the linear sweep voltammetry (LSV). In the optical screening method, the schematic is shown in Figure 2. This methodology requires an electrolyte that is a UV sensitive pH indicator. When analyzing, a constant potential is applied to the combinatorial array, which will cause catalyst spots having higher activity toward ORR to consume protons more rapidly, thus increasing the pH of the electrolyte.[27] The used electrolyte is excited under UV light when the pH is higher than 4.5;[13] therefore, the catalyst spots

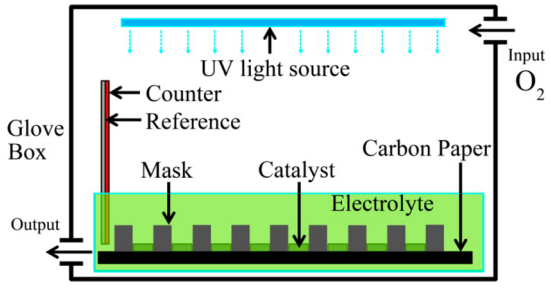

Figure 2. Scheme of the optical screening method.

with higher performance toward ORR would emit light more brightly.

For the assessment of the various catalysts by combinatorial high-throughput screening, a triangular combinatorial array for ternary compositions was prepared using the compositions shown in Figure 3a, and each spot having a different catalyst composition. To compare the ORR performance of the catalyst spots, a Pt metric catalyst was included. Each spot in the combinatorial array will be given coordinates (e.g., 1 - 1 = first line − first spot in the line) to name the spots with ease, as shown in Figure 3b. In the evaluation of the prepared combinatorial array, the two different combinatorial high-throughput methods, the multielectrode half-cell method and the optical screening method, were used. Then, the selected compositions were synthesized to single catalysts for further characterization.

RESULTS AND DISCUSSION

The prepared Pd−Ir−Ce combinatorial library was analyzed by X-ray diffraction (XRD) to verify the synthesis of the catalysts in each spot. Unfortunately, the peaks from metals did not come into view definitely because of very intense peaks from the carbon paper, which is used for the support of the combinatorial library (Supporting Information, Figure S1). Among the metals, only Pd peaks came into view (Supporting Information, Figure S2) and peaks of Ce and Ir were difficult to define. Thus, the crystalline structure of the prepared catalysts will be discussed later in the single catalyst discussion. Magnifying the XRD patterns (Supporting Information, Figure S2) from the range of 39.2 to 40.6°, it could be seen that the intensity of the Pd (111) peak diminished as the amount of Pd in the composition was decreased. Moreover, this verified that the composition of Pd was in accordance to the tendency in amount of the preparation.

The ORR analysis of the prepared Pd−Ir−Ce combinatorial library was characterized by the multielectrode half-cell method and optical screening method. In the multielectrode half-cell method, the current values for each of the 70 spots in the combinatorial array, analyzed at 0.72 V (vs. RHE), were organized in Supporting Information, Figure S3 and represented in a 2-D color graph as shown in Figure 4a. The red represents high performance and blue represents low performance toward ORR, as shown in the scale bar to the right of the 2-D graph. Pd-rich regions exhibited more red color than on Ce- or Ir-rich regions, meaning that catalyst compositions with higher performance toward ORR were near the Pd-rich regions. The spot for Pd and Pt had a current value of 0.78 and 1.39 mA, respectively, at 0.72 V (vs. RHE). Overall, six spots with the compositions 75:0:25 (1.21 mA), 77:6:17 (1.21 mA), 81:19:0 (1.21 mA), 70:13:17 (1.21 mA), 79:12:9 (1.24 mA), and 88:12:0 (1.24 mA) of Pd:Ir:Ce (at. %) had the relatively high performance toward ORR. The composition having the highest performance was the 79:12:9 at. % (Pd:Ir:Ce), with value of the current of about 1.24 mA. On the contrary, regions with the Pd percentage of about less than 50% started to show a drastic decrease in the performance toward ORR compared to Pd/C.

In the optical screening method, fluorescence images of the library were taken when a constant potential at 0.72 V (vs. RHE) was applied. Spots emitting brighter light represent catalysts with higher performance toward ORR. The image from optical screening for the Pd−Ir−Ce array is shown in the Figure 4b. In optical screening, the region with Pd-rich

dx.doi.org/10.1021/co400008v | ACS Comb. Sci. 2013, 15, 572−579

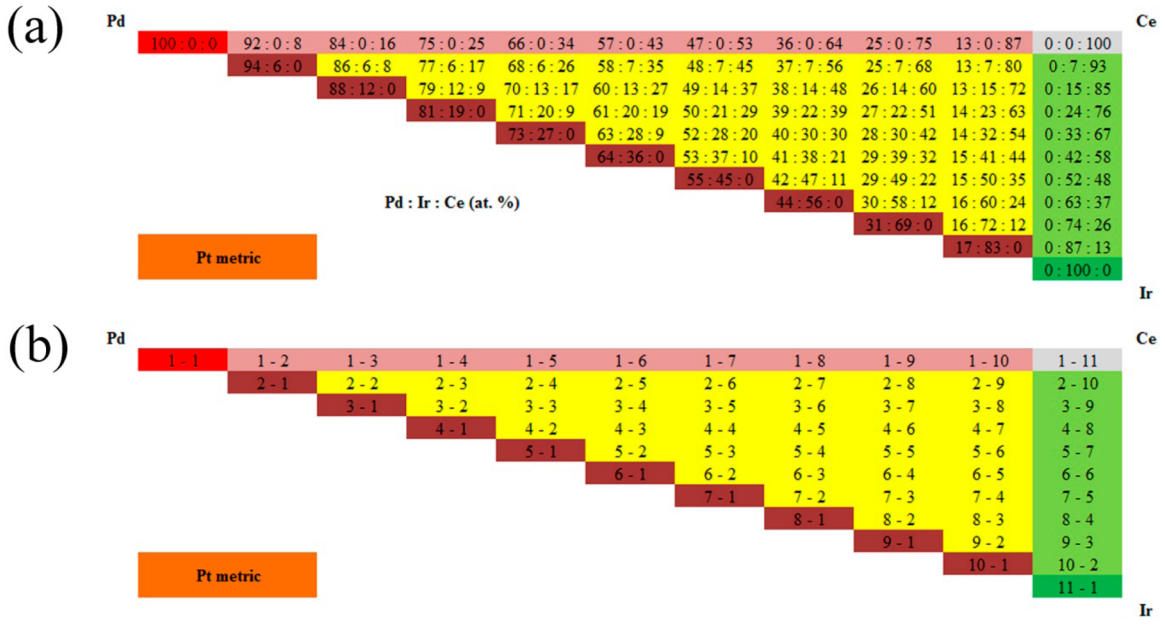

Figure 3. (a) Scheme of the compositions of combinatorial arrays for the Pd–Ir–Ce array. The ratios are expressed in Pd: Ir: Ce at. %. (b) Coordinates for each spot of the Pd–Ir–Ce array ($x - y$ = line - order). Four Pt metric catalyst spots were included at the bottom left-hand corner as a reference to the performance of the prepared catalyst spots.

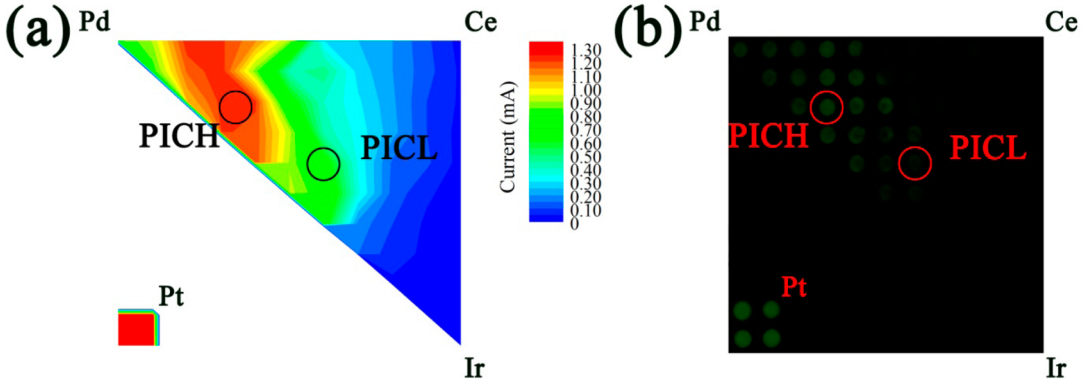

Figure 4. Combinatorial high-throughput screening of Pd–Ir–Ce library: (a) multielectrode half-cell test organized in a 2-D graph at a potential of 0.72 V (vs. RHE) and (b) optical screening test image at a constant applied potential of 0.72 V (vs. RHE). The selected compositions are labeled within the figures.

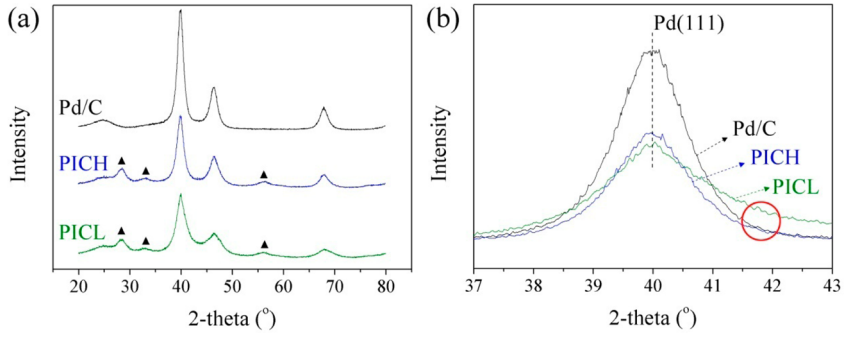

Figure 5. (a) XRD patterns of the prepared Pd-based single catalysts: Pd/C, PICH, and PICL. Triangles "▲" were used to label CeO_2 in the PICH and PICL catalysts. (b) Magnified Pd(111) peak of the prepared Pd-based catalysts at the range of 37 to 43°.

compositions in the array exhibited brighter light compared to the Ce- or Ir-rich regions, which were in accordance with the result from multielectrode half-cell test. Catalyst spots exhibiting the bright light were at compositions 75:0:25, 77:6:17, 81:19:0, 70:13:17, 70:20:9, 79:12:9, and 88:12:0 at. % (Pd:Ir:Ce), and especially the composition of 79:12:9 indicated the brightest light among the spots. However, all Pd-based catalysts exhibited less brightness compared to the Pt metric.

dx.doi.org/10.1021/co400008v | ACS Comb. Sci. 2013, 15, 572–579

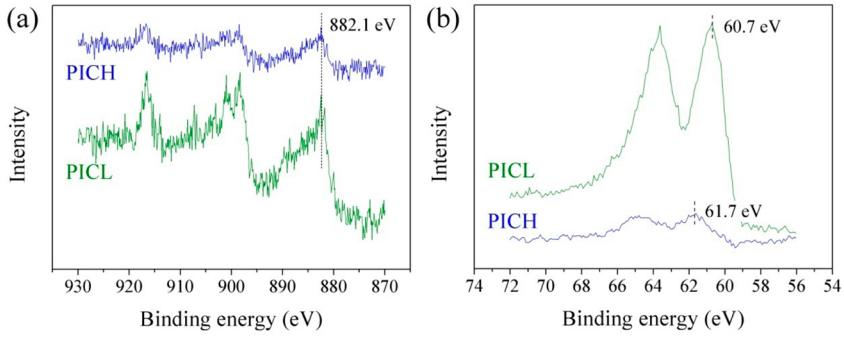

Figure 6. (a) XPS-Ce_{3d} and (b) XPS-Ir_{4f} spectroscopy of the prepared catalysts: PICH and PICL.

To verify the certification of reliability, the Pd−Ir−Ce array was examined by two different combinatorial methods (multielectrode half-cell test and optical screening), and they show similar results in ORR performance of the prepared array.

For the specific evaluation and characterization of the Pd−Ir−Ce catalyst, the composition 79:12:9 at. %, which shows the highest ORR activity from the combinatorial methods, was selected for the preparation into a single catalyst. Moreover, to examine the validity, one other catalyst composition with lower ORR performance than Pd/C was chosen (52:28:20 at. %). The single catalysts $Pd_{79}Ir_{12}Ce_9/C$ and $Pd_{52}Ir_{28}Ce_{20}/C$ will be named as PICH (Pd−Ir−Ce-High performance) and PICL (Pd−Ir−Ce-Low performance), respectively, according to their performance.

The XRD results of Pd/C, PICH, and PICL catalysts are organized in Figure 5. From the XRD patterns of the prepared catalysts, a broad peak referring to the graphite (002) facet near 25° was found for the Vulcan carbon support.[40] Moreover, clear defined peaks at around 40.1°, 46.8°, and 68.1° are assigned to the (111), (200), and (220) planes of the crystalline face cubic center (FCC) Pd lattice, respectively.[41] From the results, all three Pd peaks from the prepared catalysts did not have a definitive peak shift with respect to Pd/C (Figure 5), suggesting that alloying of Pd with other metals was not performed. In both PICH and PICL, new peaks (indicated by triangles in Figure 5a) at around 28.6°, 33.1°, and 56.4° came into view and were indexed to be of CeO_2.[42] However, clear peaks for Ir were not found. This could be due to the peak overlaps between iridium or iridium oxide peaks with that of Pd or CeO_2 XRD patterns.[41−44] From the magnification of the Pd (111) peak (Figure 5b), the PICL (with higher Ir content than PICH) tends to have a higher shoulder (indicated by a red circle in Figure 5b) compared to Pd/C or PICH, which could be due to the convolution of other peaks with intense Pd peaks (40.1°), such as Ir (40.7°) or IrO_2 (40.4°); therefore, it requires other characterizations for further statements.

X-ray photoelectron spectroscopy (XPS) analysis was performed to determine the oxidation states of Ce, Ir, and Pd of the prepared catalysts. In the case of Ce in PICH and PICL, XPS-Ce_{3d} results reveal dominant peaks at 882.1 eV, which are assigned to CeO_2 as shown in Figure 6a.[45] These results coincide with the results from XRD. In Figure 6b, XPS-Ir_{4f} results for PICH and PICL show the peaks at 61.7 and 60.7 eV, respectively. The binding energy at 60.7 eV is assigned for Ir^0 and 61.7 eV is assigned for IrO_2, deducing the state of Ir to be different in each of the prepared catalysts: IrO_2 for PICH and Ir^0 for PICL.[46,47] However, the reason for the difference in the oxidation state of Ir is unclear. Further study is required to determine the reason for the difference in the oxidation state of Ir in the prepared catalysts.

The performances toward ORR depending on the composition of the Pd-based catalysts were compared using the single catalysts, and the result is shown in Figure 7. For

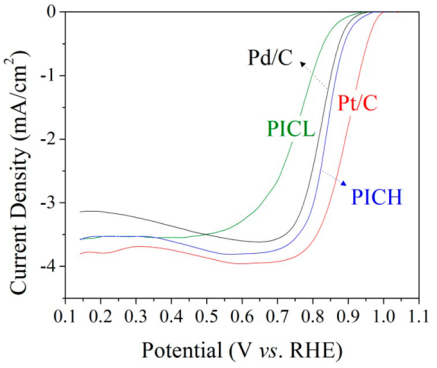

Figure 7. ORR results of the prepared Pd-based single catalysts in 1 M $HClO_4$ electrolyte: Pd/C, PICL, PICH, and Pt/C.

comparison, results for Pd/C and Pt/C were included using the same methodology as the prepared Pd−Ir−Ce catalysts were examined. The onset potentials of the prepared catalysts were 0.95 V for Pd/C, 0.97 V for PICH, 0.94 V for PICL, and 1.03 for Pt/C. The results from electrochemical characterizations of the prepared catalysts were organized in Table 1. The values of current density of the prepared catalysts at a potential of 0.85 V (vs. RHE) were collected to compare the ORR performance. The current densities were in the order of PICL (−0.30 mA/cm^2) < Pd/C (−1.02 mA/cm^2) < PICH (−1.50 mA/cm^2) < Pt/C (−2.94 mA/cm^2). Pd/C shows a much lower ORR activity compared to that of Pt/C; however, PICH shows a significantly improved ORR performance compared with that of Pd/C. PICL shows lower ORR activity than that of Pd/C in the single catalyst evaluation, and this result is in accordance with that of the combinatorial results. The tendency toward the ORR activity of the prepared catalysts was similar to the tendency found from the combinatorial high-throughput method.

The mass activities of Pd/C, PICH, and PICL at 0.85 V (vs. RHE) were calculated and that of Pt/C was included for comparison. The mass activities derived from the kinetic current density, based on only Pd or Pt amounts, were Pd/C (−8.85 mA/$mg_{of\ Pd}$), Pt/C (−42.50 mA/$mg_{of\ Pt}$), PICH (−27.57 mA/$mg_{of\ Pd}$), and PICL (−5.43 mA/$mg_{of\ Pd}$). The mass activity of PICH catalyst was about 3.1 times higher than

dx.doi.org/10.1021/co400008v | ACS Comb. Sci. 2013, 15, 572−579

Table 1. Electrochemical Properties of the Prepared Catalysts

sample	metal loading (wt %)	Pd:Ir:Ce[a] (at. %)	Pd:Ir:Ce[b] (at. %)	E_{onset} (V)	J^c (mA/cm^2)	$J_k{}^c$ (mA/cm^2)	M.A.[c,d] (mA/mg)
Pt/C	40.0			1.03	−2.94	−11.50	−42.50
Pd/C	38.5			0.95	−1.02	−1.43	−8.85
PICH	35.1	79:12:9	84:10:6	0.97	−1.50	−2.48	−19.30
PICL	37.6	52:28:20	52:29:19	0.94	−0.30	−0.32	−2.17

[a]Stoichiometric value. [b]Obtained from ICP analysis. [c]Calculated at 0.85 V (vs RHE). [d]Mass activity based on noble metals.

that of Pd/C; however, it still shows lower activity than that of Pt/C. The order of mass activities based on Pd or Pt amounts was in the order of PICL < Pd/C < PICH < Pt/C. However, as Ir is also a noble metal, the presence of this metal could not be discarded; therefore, the mass activity based on both Pd and Ir was calculated for the ternary catalysts. As shown in Table 1, the mass activities of the prepared catalysts were calculated when both Pd and Ir were considered, and they were PICL (-2.17 mA/mg$_{\text{of Pd and Ir}}$) and PICH (-19.30 mA/mg$_{\text{of Pd and Ir}}$). The performance of PICH catalyst was about 2 times the mass activity of Pd/C. The order of performance was verified to be PICL < Pd/C < PICH < Pt/C, and in both cases, the mass activities of PICH were higher than that of Pd/C.

It is proposed that the enhanced ORR activity of PICH is due to the electron-modification of Pd active sites. Figure 8

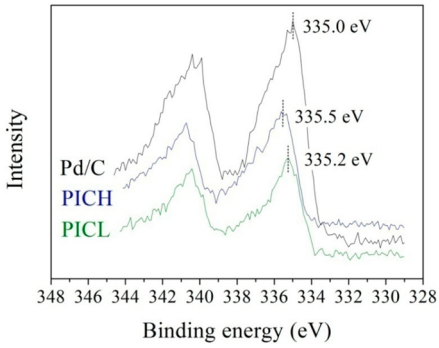

Figure 8. XPS-Pd$_{3d}$ spectroscopy of the prepared catalysts: Pd/C, PICH, and PICL.

shows XPS-Pd$_{3d}$ results of the prepared catalysts. The binding energies of Pd for Pd/C, PICH, and PICL were found at 335.0, 335.5, and 335.2 eV respectively. The Pd binding energies of the PICH catalyst are up-shifted by 0.5 eV compared to that of Pd/C, respectively. This upshift of the XPS-Pd$_{3d}$ peak indicates the electron modification of the Pd particles. Moreover, Lewera et al. reported the enhancement of ORR activity of Pt, via TiO_2 and WO_3 decoration, was due to the increased electron density of Pt.[48] Zhang et al. mentioned that the strong metal−metal oxide interaction between Pd and WO_3 causes the electron modification of Pd particles, which was shown by the shift of XPS-Pd$_{3d}$ peak of Pd-WO_3/C.[49] Our previous study also revealed enhancement of ORR activity through the modification of electron densities of noble metals via strong metal−metal oxide interaction, which changed the bonding strength between the reactants and the active sites (noble metals).[50] The peak shifts of XPS-Pd$_{3d}$ for PICH, shown in Figure 8, could indicate a strong metal (Pd)−transition metal oxide (IrO_2 or CeO_2) interaction.

The upshift from the XPS-Pd$_{3d}$ in PICH implies a decrease in energy of the d-band center, which would reduce the oxygen-active site adsorption energy. This decrease in adsorption of oxygen molecules to the Pd particles could have had an effect on the increase in ORR activity. Even though PICL also indicates a 0.2 eV upshift of binding energy in XPS-Pd$_{3d}$; however, it shows a lower ORR activity compared to that of Pd/C, and this might be due to the sluggish electron transfer to the active site induced by increased amount of CeO_2, which acted as an insulator. A similar phenomenon has been observed in previous studies,[50] where the decoration of metal particles with metal oxide increased the ORR activity, but the presence of excess metal oxide prohibited the facile electron transfer resulting in the decrease of ORR activity.

In conclusion, a total of 66 different combinations of Pd-based ternary catalysts were investigated as non-Pt catalysts for ORR in acid media using combinatorial high-throughput methods. By using two different high-throughput methods, multielectrode half-cell test and optical screening, the performance of various compositions were evaluated simultaneously and confirmed for their validity. The chosen composition with the highest performance toward ORR in the Pd−Ir−Ce combinatorial array was the 79:12:9 at. %. From the single catalyst analysis, optimized Pd−Ir−Ce catalyst demonstrates a 2 times higher mass activity compared with that of Pd/C. XPS results reveal that electron modification of Pd induced by a strong metal (Pd)−transition metal oxide (IrO_2 or CeO_2) interaction is responsible for improved ORR activity of the Pd−Ir−Ce catalyst. In the selection of optimum composition for highly active Pd-based catalysts, combinatorial methods proved to support each other in the evaluation for the performance of the catalysts toward ORR. Such methodologies would be very useful for the future when vast variations of different combinations and compositions are analyzed to find the optimum choice.

EXPERIMENTAL PROCEDURES

In the combinatorial array 66 spots were imprinted on a polytetrafluoroethylene (PTFE) treated carbon paper (Toray TGPH−090, 20 wt % PTFE) by spraying a carbon ink using a spray and a designed stainless-steel mask with the adequate dimensions.[3,13,38,39] Each carbon spot had a diameter of 4 mm and a mass of 0.15 mg. The carbon ink was prepared by a mixture of Vulcan XC-72R (0.1 g), deionized (DI) water (120 μL), 5 wt % Nafion ionomer solution (970 μL), and isopropyl alcohol (5 mL, IPA, Aldrich). The carbon ink is necessary because the carbon paper is treated with PTFE, so it is hydrophobic. Without the added carbon ink support, the metals would not be well dispersed. The use of carbon ink also helps prepare the catalysts on the inked spots in the combinatorial array to be as similar as possible to the bulk powder catalysts. Moreover, the use of the carbon ink helps ensure that the catalyst spots all have the same area, making comparison of absolute currents more valid. After imprinting the carbon spots on the carbon paper, the catalyst precursor solutions were dropped using a pipet at each carbon spot. For the various compositions of the catalyst spots, the metal precursors were prepared in solutions. Palladium nitrate ($Pd(NO_3)_2{\cdot}xH_2O$,

dx.doi.org/10.1021/co400008v | ACS Comb. Sci. 2013, 15, 572−579

Aldrich), iridium chloride ($IrCl_3 \cdot 3H_2O$, Aldrich), and cerium chloride ($CeCl_3 \cdot 7H_2O$, Aldrich), were used as metal precursors. After the loading of appropriate catalyst solutions on each carbon spot, the library was dried at room temperature. The total metal loading on carbon was adjusted to 40 wt %. Then the metal precursors on the combinatorial library were reduced using 0.2 M $NaBH_4$ solution. To compare the ORR performance of the Pd-based catalyst spots, 4 additional catalyst spots of commercial Pt/C (40 wt %) from E-tek were included on the left bottom corner of the combinatorial library. A calculated amount Pt/C was also sprayed using a Pt/C ink. The Pt/C ink was prepared by a mixture of commercial Pt/C (40 wt %, 0.17 g, E-tek), deionized (DI) water (120 μL), 5 wt % Nafion ionomer solution (970 μL), and isopropyl alcohol (5 mL, IPA, Aldrich). The combinatorial libraries were characterized by both the multi electrode half-cell method,[3] and the optical screening method.[39] In all the electrochemical tests including combinatorial and single catalyst study, a platinum wire (ALS Co., 002233) and an Ag/AgCl electrode (ALS CO., 012167) were used as counter and reference electrodes, respectively. All electrochemical tests were done using an electrochemical analyzer (CH Instruments, Inc. CHI700D). In this paper, all the potential scales have been converted to reversible hydrogen electrode (RHE) for convenience.

The Multielectrode half-cell method is similar to the three electrode half-cell test, consisting of a working, a counter, and a reference electrode. In this methodology, the prepared combinatorial library was used as working electrode. For the activation of the combinatorial library, 30 cycles of cyclic voltammetry (CV), at a range between 0 to 0.798 V (vs RHE), was conducted in deaerated 1 M $HClO_4$ electrolyte with a 15 mV/s scan rate. To measure the ORR activity of each catalyst composition, a PTFE mask with 70 holes (each hole on each catalyst spot on the combinatorial library) of 5 mm diameter and 10 mm depth is used for electrolyte isolation. To measure the ORR activity of each composition, the counter and reference electrodes were put into each hole. This process was repeated for each and every spot on the library. The ORR was analyzed by a single linear sweep between 1.04 to 0.14 V (vs. RHE) at an oxygen purged 1 M $HClO_4$ electrolyte with a 5 mV/s scan rate. The total time to conduct all the LSV of the catalyst spots was 210 min (in the case of this experiment). However, this factor can be altered depending on the range of the LSV analysis. For example, if the needed current value is at around a specific potential, for example, at 0.75 V (vs RHE), the range of screening can be shortened from 1.04−0.14 V to 1.04−0.59 V (vs RHE). This would shorten the total time of analysis from 210 min to half its time (105 min). In conclusion, the total time of analysis can be altered depending on the range of LSV.

In optical screening, the combinatorial array was used as the working electrode in a three electrode half-cell test. The electrolyte was prepared with 100 μM fluorescein sodium salt (Aldrich) and 0.2 M $NaNO_3$ (Aldrich). Fluorescein was selected as the pH indicator for the evaluation of ORR performance of the catalyst spots in the combinatorial array according to previous reports.[13,39] $NaNO_3$ was included as a conduction supporting agent, which reduces the conduction resistance in the electrolyte. This solution was adjusted to pH of 4 using $HClO_4$ and NaOH solutions. The solution was purged with pure oxygen for 2 h before usage. Optical screening was then carried out inside a homemade glovebox, which contains a UV light source and a camera, where images could be taken in a dark environment. For the activation of the combinatorial library, 30 cycles of CV at a range between 0 to 0.798 V (vs RHE) were conducted in deaerated 1 M $HClO_4$ electrolyte with a 15 mV/s scan rate, same as in the multielectrode half-cell method. A homemade mask with the same dimensions as the PTFE mask from the multielectrode half-cell was prepared for optical screening using Bakelite material. This optical screening mask was made to decrease the diffusion and mixture between the electrolytes on each spot. Using the potentiostat/galvanostat system in the electrochemical analyzer, a constant potential of 0.72 V (vs. RHE) was applied onto the combinatorial array under UV light. The applied potential (0.72 V vs. RHE) was chosen as the potential at which the ORR performance results from the two combinatorial methods were to be compared. Images were taken under UV light to excite the fluorescence emitted by the indicator, and the image taken after 15 min was selected for analysis. If the brightness is too difficult to differentiate between the spots with the naked eye, then a program like Adobe Photoshop can be used to more accurately identify the spots emitting brighter light.

XRD patterns of the combinatorial array were acquired using a Combinatorial microbeam XRD (Bruker-AXS) operating a 40 kV and 40 mA, with step-scan patterns between 17.7 to 78.7° (2θ range) with 0.1° step size and 2°/min scan speed.

The chosen compositions from the Pd−Ir−Ce combinatorial array, $Pd_xIr_yCe_z/C$, were synthesized by an impregnation method using $NaBH_4$ reduction, which is a similar method to the preparation of the combinatorial array (Method 2.1). The same metal precursors were used in the synthesis. The carbon support (Vulcan XC-72R, 0.1 g) was dispersed in a mixture of 200 mL of DI-water and 100 mL of IPA, using an ultrasonicator. Then the calculated amounts of the metal precursors were added to the solution and stirred for 30 min. The calculations were fixed in atomic percent of the metal being loaded, and the values were Pd:Ir:Ce = 79:12:9 and 52:28:20 (at. %). The chemical reduction of the metal precursors was performed by adding calculated amounts of $NaBH_4$ (the mole of total metal precursors ×10) dissolved in 100 mL of DI-water into the solution. This mixture was then stirred for 2 h for the reduction of metal precursors. The mixture was then, filtered, washed with DI-water, and dried in an oven at 80 °C overnight. Pd/C was also prepared using the same method for comparison and reference. In all the prepared catalysts, the metal loading was adjusted to 40 wt % of the total catalyst mass. Pt/C (40 wt %, E-tek) was also used for comparison and reference.

Physical characterizations of the single catalysts were performed by transmission electron spectroscopy (TEM), XRD, and XPS. TEM images were taken with a JEM2100-F (Jeol Ltd.) operated at 200 kV. XRD patterns were acquired using a D/MAX-2500 (RIgaku) operating a 40 kV and 300 mA, with step-scan patterns between 20 to 80° (2θ range) with 0.01° step size and 1°/min scan speed. XPS analysis were tested using a Sigma Probe (Thermo VG Scientific) equipped with a microfocused monochromator X-ray source.

Electrochemical properties were analyzed using a three-electrode-type beaker cell equipped with a counter electrode, a reference electrode, and a rotating disk electrode (ALS Co., 011169, diameter = 3 mm), using a rotator (ALS Co., RRDE-3A). The working electrodes were prepared by the thin-film electrode method. The catalysts (10 mg, carbon supported samples) were dispersed in ink solution (1 mL; DI-water (15),

dx.doi.org/10.1021/co400008v | ACS Comb. Sci. 2013, 15, 572−579

5 wt % Nafion in water (4), and isopropyl alcohol (1); the number in parentheses indicates the volumetric ratio) followed by sonication, and then the catalyst inks (5 μL) were dropped onto a glassy carbon of a rotating ring disk electrode. The catalyst inks were dried at room temperature. Thirty cycles of the CV experiments were conducted in deaerated 1 M $HClO_4$ electrolyte for activation of the catalysts with a 15 mV/s scan rate from 0 to 0.798 V (vs. RHE). The ORR experiments were conducted in O_2 saturated 1 M $HClO_4$ electrolyte with a 5 mV/s scan rate and 2000 rpm rotating velocity from 1.04 to 0.14 V (vs. RHE). Kinetic current from the ORRs was derived from the following equation:

$$\frac{1}{J} = \frac{1}{J_k} + \frac{1}{J_d} \quad (1)$$

where J is a current from ORR in LSV experiments, J_k is a kinetic current, and J_d is a diffusion current. The mass activity of the catalyst was calculated from the kinetic current at 0.85 V (vs RHE).

■ ASSOCIATED CONTENT

Supporting Information

XRD results of the combinatorial array, and ORR results of the combinatorial half-cell test. This material is available free of charge via the Internet at http://pubs.acs.org.

■ AUTHOR INFORMATION

Corresponding Author

*E-mail: siwoo@kaist.ac.kr.

Funding

This work was supported by the Samsung Advanced Institute of Technology (SAIT, SAMSUNG ELECTRONICS Co., Ltd) and the National Research Foundation of Korea (NRF) grant funded by the Korea government (MEST) (No. 2009-0092783).

Notes

The authors declare no competing financial interest.

■ ABBREVIATIONS

PICH, $Pd_{79}Ir_{12}Ce_9/C$; PICL, $Pd_{52}Ir_{28}Ce_{20}/C$

■ REFERENCES

(1) Brumfiel, G. Hydrogen Cars Fuel Debate on Basic Research. *Nature* **2003**, *422*, 104−104.

(2) Jacobson, M. Z.; Colella, W. G.; Golden, D. M. Cleaning the Air and Improving Health with Hydrogen Fuel-Cell Vehicles. *Science* **2005**, *308*, 1901−1905.

(3) Lee, K. R.; Jung, Y.; Woo, S. I. Combinatorial Screening of Highly Active Pd Binary Catalysts for Electrochemical Oxygen Reduction. *ACS Comb. Sci.* **2012**, *14*, 10−16.

(4) Zhang, L.; Lee, K.; Zhang, J. J. The Effect of Heat Treatment on Nanoparticle Size and ORR Activity for Carbon-Supported Pd-Co Alloy Electrocatalysts. *Electrochim. Acta* **2007**, *52*, 3088−3094.

(5) Li, X. W.; Huang, Q. H.; Zou, Z. Q.; Xia, B. J.; Yang, H. Low Temperature Preparation of Carbon-Supported Pd-Co Alloy Electrocatalysts for Methanol-Tolerant Oxygen Reduction Reaction. *Electrochim. Acta* **2008**, *53*, 6662−6667.

(6) Ramos-Sanchez, G.; Yee-Madeira, H.; Solorza-Feria, O. PdNi Electrocatalyst for Oxygen Reduction in Acid Media. *Int. J. Hydrogen Energy* **2008**, *33*, 3596−3600.

(7) Shao, M. H.; Sasaki, K.; Adzic, R. R. Pd-Fe Nanoparticles as Electrocatalysts for Oxygen Reduction. *J. Am. Chem. Soc.* **2006**, *128*, 3526−3527.

(8) Sarkar, A.; Murugan, A. V.; Manthiram, A. Synthesis and Characterization of Nanostructured Pd-Mo Electrocatalysts for Oxygen Reduction Reaction in Fuel Cells. *J. Phys. Chem. C* **2008**, *112*, 12037−12043.

(9) Kim, I. T.; Choi, M.; Lee, H. K.; Shim, J. Characterization of Methanol-Tolerant Pd-WO_3 and Pd-SnO_2 Electrocatalysts for the Oxygen Reduction Reaction in Direct Methanol Fuel Cells. *J. Ind. Eng.Chem.* **2012**, *19*, 813−818.

(10) Maheswari, S.; Sridhar, P.; Pitchumani, S. Pd-TiO_2/C as a Methanol Tolerant Catalyst for Oxygen Reduction Reaction in Alkaline Medium. *Electrochem. Commun.* **2013**, *26*, 97−100.

(11) Kwon, K.; Lee, K. H.; Jin, S. A.; You, D. J.; Pak, C. Ceria-Promoted Oxygen Reduction Reaction in Pd-Based Electrocatalysts. *Electrochem. Commun.* **2011**, *13*, 1067−1069.

(12) Choi, C. H.; Park, S. H.; Woo, S. I. Oxygen Reduction Activity of Pd-Mn_3O_4 Nanoparticles and Performance Enhancement by Voltammetrically Accelerated Degradation. *Phys. Chem. Chem. Phys.* **2012**, *14*, 6842−6848.

(13) Liu, J. H.; Jeon, M. K.; Woo, S. I. High-Throughput Screening of Binary Catalysts for Oxygen Electroreduction. *Appl. Surf. Sci.* **2006**, *252*, 2580−2587.

(14) Kang, S.; Park, S.; Kim, K. W.; Woo, S. I.; Park, S. High-Throughput Screening of Ferroelectric Materials for Non-Volatile Random Access Memory Using Multilayer Perceptrons. *Appl. Surf. Sci.* **2007**, *254*, 725−733.

(15) Oh, K. S.; Woo, S. I. Chemiluminescence Analyzer of NO_x as a High-Throughput Screening Tool in Selective Catalytic Reduction of NO. *Sci. Technol. Adv. Mater.* **2011**, *12*, 1−7.

(16) Lee, W. S.; Kim, T. Y.; Woo, S. I. High-Throughput Screening for the Promoters of Alumina Supported Ni Catalysts in Autothermal Reforming of Methane. *Top. Catal.* **2010**, *53*, 123−128.

(17) Woo, S. I.; Kim, S. H. Combinatorial Science and High-Throughput Experiments for Catalysis. *Top. Catal.* **2010**, *53*, 1−1.

(18) Kim, K. W.; Jeon, M. K.; Kim, T. S.; Oh, K. S.; Shin, J. W.; Woo, S. I. Quantitative Structure-Property Relationship in a Combinatorial Bi_4-$xLa_xTi_3O_{12}$ ($0 \leq x \leq 1$) Thin Film Array Obtained with Microbeam XRD and Raman Spectroscopy. *J. Comb. Chem.* **2007**, *9*, 823−827.

(19) Oh, K. S.; Woo, S. I. Effect of Preparation and Reaction Condition on the Catalytic Performance of Mo-V-Te-Nb Catalysts for Selective Oxidation of Propane to Acrylic Acid by High-Throughput Methodology. *Catal. Today* **2008**, *137*, 61−70.

(20) Kim, K. W.; Jeon, M. K.; Oh, K. S.; Kim, T. S.; Kim, Y. S.; Woo, S. I. Combinatorial Approach for Ferroelectric Material Libraries Prepared by Liquid Source Misted Chemical Deposition Method. *Proc. Natl. Acad. Sci. U.S.A.* **2007**, *104*, 1134−1139.

(21) Noh, J.; Suh, Y. D.; Park, Y. K.; Jin, S. M.; Kim, S. H.; Woo, S. I. Combined Micro-Raman/UV-Visible/Fluorescence Spectrometer for High-Throughput Analysis of Microsamples. *Rev. Sci. Instrum.* **2007**, *78*, 1−6.

(22) Woo, S. I.; Kim, K. W.; Cho, H. Y.; Oh, K. S.; Jeon, M. K.; Tarte, N. H.; Kim, T. S.; Mahmood, A. Current Status of Combinatorial and High-Throughput Methods for Discovering New Materials and Catalysts. *QSAR Comb. Sci.* **2005**, *24*, 138−154.

(23) Oh, K. S.; Park, Y. K.; Woo, S. I. Highly Reliable 64-Channel Sequential and Parallel Tubular Reactor System for High-Throughput Screening of Heterogeneous Catalysts. *Rev. Sci. Instrum.* **2005**, *76*, 1−7.

(24) Choi, W. C.; Jeon, M. K.; Kim, Y. J.; Woo, S. I.; Hong, W. H. Development of Enhanced Materials for Direct-Methanol Fuel Cell by Combinatorial Method and Nanoscience. *Catal. Today* **2004**, *93*−*5*, 517−522.

(25) Cho, H. Y.; Hong, D. S.; Jeong, D. W.; Gong, Y. D.; Woo, S. I. High-Throughput Synthesis of New Ni(II), Pd(II), and Co(II) Catalysts and Polymerization of Norbornene Utilizing the Self-Made Parallel Polymerization Reactor System. *Macromol. Rapid Commun.* **2004**, *25*, 302−306.

(26) Choi, W. C.; Kim, Y. J.; Woo, S. I.; Hong, W. H. Improving Direct Methanol Fuel Cell Performance by Using Combinatorial

Electrochemistry and Highly Porous Carbon Support. *Stud. Surf. Sci. Catal.* **2003**, *145*, 395−398.
(27) Reddington, E.; Sapienza, A.; Gurau, B.; Viswanathan, R.; Sarangapani, S.; Smotkin, E. S.; Mallouk, T. E. Combinatorial Electrochemistry: A Highly Parallel, Optical Screening Method for Discovery of Better Electrocatalysts. *Science* **1998**, *280*, 1735−1737.
(28) Chan, B. C.; Liu, R. X.; Jambunathan, K.; Zhang, H.; Chen, G. Y.; Mallouk, T. E.; Smotkin, E. S. Comparison of High-Throughput Electrochemical Methods for Testing Direct Methanol Fuel Cell Anode Electrocatalysts. *J. Electrochem. Soc.* **2005**, *152*, A594−A600.
(29) Chen, G. Y.; Delafuente, D. A.; Sarangapani, S.; Mallouk, T. E. Combinatorial Discovery of Bifunctional Oxygen Reduction - Water Oxidation Electrocatalysts for Regenerative Fuel Cells. *Catal. Today* **2001**, *67*, 341−355.
(30) Cooper, J. S.; McGinn, P. J. Combinatorial Screening of Thin Film Electrocatalysts for a Direct Methanol Fuel Cell Anode. *J. Power Sources* **2006**, *163*, 330−338.
(31) Gurau, B.; Viswanathan, R.; Liu, R. X.; Lafrenz, T. J.; Ley, K. L.; Smotkin, E. S.; Reddington, E.; Sapienza, A.; Chan, B. C.; Mallouk, T. E.; Sarangapani, S. Structural and Electrochemical Characterization of Binary, Ternary, and Quaternary Platinum Alloy Catalysts for Methanol Electro-Oxidation. *J. Phys. Chem. B* **1998**, *102*, 9997−10003.
(32) Morris, N. D.; Mallouk, T. E. A High-Throughput Optical Screening Method for the Optimization of Colloidal Water Oxidation Catalysts. *J. Am. Chem. Soc.* **2002**, *124*, 11114−11121.
(33) Prochaska, M.; Jin, J.; Rochefort, D.; Zhuang, L.; DiSalvo, F. J.; Abruna, H. D.; van Dover, R. B. High Throughput Screening of Electrocatalysts for Fuel Cell Applications. *Rev. Sci. Instrum.* **2006**, *77*, 1−8.
(34) Smotkin, E. S.; Diaz-Morales, R. R. New Electrocatalysts by Combinatorial Methods. *Ann. Rev. Mater. Res.* **2003**, *33*, 557−579.
(35) Smotkin, E. S.; Jiang, J. H.; Nayar, A.; Liu, R. X. High-Throughput Screening of Fuel Cell Electrocatalysts. *Appl. Surf. Sci.* **2006**, *252*, 2573−2579.
(36) Sun, Y. P.; Buck, H.; Mallouk, T. E. Combinatorial Discovery of Alloy Electrocatalysts for Amperometric Glucose Sensors. *Anal. Chem.* **2001**, *73*, 1599−1604.
(37) Gurau, B.; Viswanathan, R.; Liu, R. X.; Lafrenz, T. J.; Ley, K. L.; Smotkin, E. S.; Reddington, E.; Sapienza, A.; Chan, B. C.; Mallouk, T. E.; Sarangapani, S. Structural and Electrochemical Characterization of Binary, Ternary, and Quaternary Platinum Alloy Catalysts for Methanol Electro-Oxidation. *J. Phys. Chem. B* **1998**, *102*, 9997−10003.
(38) Lee, K. R.; Jeon, M. K.; Woo, S. I. Composition Optimization of PtRuM/C (M = Fe and Mo) Catalysts for Methanol Electro-Oxidation Via Combinatorial Method. *Appl. Catal., B* **2009**, *91*, 428−433.
(39) Jeon, M. K.; Liu, J. H.; Lee, K. R.; Lee, J. W.; McGinn, P. J.; Woo, S. I. Combinatorial Search for Quaternary Methanol Tolerant Oxygen Electro-Reduction Catalyst. *Fuel Cells* **2010**, *10*, 93−98.
(40) Maiyalagan, T.; Khan, F. N. Electrochemical Oxidation of Methanol on Pt/V_2O_5-C Composite Catalysts. *Catal. Commun.* **2009**, *10*, 433−436.
(41) Yeh, Y. C.; Chen, H. M.; Liu, R. S.; Asakura, K.; Lo, M. Y.; Peng, Y. M.; Chan, T. S.; Lee, J. F. Pd-C-Fe Nanoparticles Investigated by X-Ray Absorption Spectroscopy as Electrocatalysts for Oxygen Reduction. *Chem. Mater.* **2009**, *21*, 4030−4036.
(42) Snell, R. W.; Shanks, B. H. Ceria Calcination Temperature Influence on Acetic Acid Ketonization: Mechanistic Insights. *Appl. Catal., A* **2013**, *451*, 86−93.
(43) Lee, K.; Zhang, L.; Zhang, J. J. Ir_xCo_{1-x} (x = 0.3−1.0) Alloy Electrocatalysts, Catalytic Activities, and Methanol Tolerance in Oxygen Reduction Reaction. *J. Power Sources* **2007**, *170*, 291−296.
(44) Negi, S.; Bhandari, R.; Rieth, L.; Solzbacher, F. Effect of Sputtering Pressure on Pulsed-DC Sputtered Iridium Oxide Films. *Sens. Actuators, B* **2009**, *137*, 370−378.
(45) Barr, T. L. An Esca Study of the Termination of the Passivation of Elemental Metals. *J. Phys. Chem.* **1978**, *82*, 1801−1810.
(46) Hufner, S.; Wertheim, G. K.; Wernick, J. H. XPS Core Line Asymmetries in Metals. *Solid State Commun.* **1975**, *17*, 417−422.
(47) Zhao, C.; Yu, H.; Li, Y.; Li, X.; Ding, L.; Fan, L. Electrochemical Controlled Synthesis and Characterization of Well-Aligned Iro_2 Nanotube Arrays with Enhanced Electrocatalytic Activity toward Oxygen Evolution Reaction. *J. Electroanal. Chem.* **2013**, *688*, 269−274.
(48) Lewera, A.; Timperman, L.; Roguska, A.; Alonso-Vante, N. Metal-Support Interactions between Nanosized Pt and Metal Oxides (WO_3 and TiO_2) Studied Using X-Ray Photoelectron Spectroscopy. *J. Phys. Chem. C* **2011**, *115*, 20153−20159.
(49) Zhang, C.; Boudiba, A.; Olivier, M.-G.; Snyders, R.; Debliquy, M. Sensing Properties of Pt/Pd Activated Tungsten Oxide Films Grown by Simultaneous Radio-Frequency Sputtering to Reducing Gases. *Sens. Actuators, B* **2012**, *175*, 53−59.
(50) Jeon, M. K.; Lee, K. R.; Woo, S. I. Enhancement in Electro-Oxidation of Methanol over PtRu Black Catalyst through Strong Interaction with Iron Oxide Nanocluster†. *Langmuir* **2010**, *26*, 16529−16533.